Geospatial Analysis of COVID-19 Spread in Cairo Governorate Using Geographic Information System

Shimaa Abd Elnaby*
Asmaa Al Qersh**

ABSTRACT

COVID-19 has caused a global public health crisis affecting most countries including Egypt Due to the widespread pandemic; the spread of COVID-19 has drawn increasing global attention. This study aims to analyze the reported Covid-19 cases by spatial statistical methods, exploring the geographical distribution patterns of the COVID-19 pandemic in Cairo from 14 February 2020 to 18 of May 2021. In order to better understand of the spread of this new virus, The spatial patterns of Covid-19 cumulative cases have been characterized by using ArcGIS ver. 10.3.1 based on spatial autocorrelation and cluster analysis using Global Moran's I (Moran, 1950), Local Moran's I and Getis-Ord Gi to explore the spatial gathering hotspots and cold spots of the COVID-19 pandemic .Up to 18 may 2021, Cairo Province had reported 79,130 Covid-19 cases. The top five districts with respect to incidence were Al Mouski (0.097/100000), Badr (0.088/100000), Qasr Al niel (0.088/100000), Al Gammalia (0.066/100000) and Al Zamalek (0.064/100000). Global Moran's I analysis results showed that the Morbidity rate, recovery and fatality of COVID19 was in the clustering pattern, and there was less than 1% likelihood that this clustering pattern could be the result of random chance. While local spatial correlation analysis showed that the value of 71 sheikhs belonging to the HH aggregation class. The Getis -OrdGi statistic was applied and the results showed that the clustering of high values (hot spots) for Morbidity with a confidence level of 99% distributed in eastern, southern and the northeast of Cairo. **[Bul. Soc. Géog. d'Égypte, 2021, 94: 24-43]**

Key Words: COVID-19, GIS, Spatial autocorrelation, Hot/cold spots, Cairo.

1. Introduction

COVID-19 has become one of the most serious global public health crises in modern times. The disease was declared a pandemic on 11 March 2020 and has currently affected more than 216 countries and territories (Cucinotta, 2020). As of 3 August 2020, there were more than 17.6 million confirmed COVID-19 cases and over 680 000 associated deaths around the globe (WHO, 2020). A key element of epidemiologic research, the geographical distribution of the disease, is demonstrated by the importance

* Lecturer of Human Geography, Faculty of Arts - Alexandria University, Egypt.
** Lecturer of Physical Geography, Faculty of Arts - Alexandria University, Egypt.
For Correspondence: e-mail: s.abdelnaby@alexu.edu.eg; asmaa.elkersh@alexu.edu.

given to the ‘‘person, place and time’’ descriptor of health events in the classical epidemiology textbooks (Werneck, 2008). This thematic aspect of COVID-19 requires analysis that adopts an interdisciplinary approach, and geography is one of the few disciplines that purports to offer a synthetic approach to the interplay between the biophysical and human variables (Turner, 2002), by approaching the environment from a holistic perspective with a focus on the forms and processes that concur in a geographical space (Sauer, 1925). Other disciplines define the physical, historical and social characteristics and processes, but geography situates these in a spatial, territorial, locational and landscape perspective (Pattison, 1964). The complex reality of the environment-society dialectic must be understood in the context of the integrative approach of geography .Geographical information systems (GIS) have today revolutionized these spaces-which, in simple terms, give the ability to view spatial or geographic information in a meaningful way, be it interactive maps or other infographics. There are numerous uncertainties in the Covid pandemic, many of them have a spatial component that contributes to the pandemic being interpreted as geographical and technically mappable (Subramanian et al., 2020) .In the battle against Covid in Cairo, there have been limited Covid risk maps and application of Covid spatial epidemiology. For these purposes, with the emergence of Covid as a global pandemic, the use of geospatial and statistical methods has become extremely important. Statistical modeling and spatial epidemiology in small areas have been developed to solve problems where disease clusters and hotspots are located (Franch-Pardo et al., 2020). Some of the principal spatial techniques explored by Robertson (Robertson et al., 2014) are spatial autocorrelation, spatial time interactions, hotspots, and clusters, used throughout emerging infectious disease research. Advances in geostatistical methods have provided for substantially improved efficiency in the processing and analysis of complex geo-referenced data with multiple variables on different geographical scales, providing epidemiologists with new instruments to incorporate space and place in their study. Based on the numbers available, we demonstrate in this paper spatial cluster patterns of Covid-19 inside Cairo, information that should prove useful for improved, future control of the pandemic.

2. Materials and Methods

2.1 Study Area

Cairo is the largest city in Egypt and the country's capital. It is located on the Eastern bank of the Nile, Cairo is a governorate and a city. Cairo bordered from the north by Qalyobia governorate and from the eastern and southern sides by the desert hinterland, and from the western side by the River Nile and Giza Governorate. Cairo, the largest city in Africa, is located on the Nile River, 160 kilometers (100 miles) inland from the Mediterranean

Sea and 135 kilometers (80 miles) west of the Red Sea as showed in figure (1). The total area of Cairo reaches (3085.10) km^2. The inhabited area reaches about (190.42) km^2. Cairo is the largest governorate all over the Republic in terms of population. The total population is estimated to 9. 539. 673 up to 2017 according to the Central Agency for Public Mobilization and Statistics, Egypt, representing approximately 10.6% of Egypt's total population. The arithmetic density of population reaches (46.86 inhabitants / km2). Cairo consists of four regions comprising (46) districts divided into 325 sheikhs "according to the latest amendment of the administrative boundaries of Cairo governorate in 2021". The main four regions of Cairo divided as follows: The northern region comprises (8) districts, the eastern region includes (14) districts the western region includes (12) districts and the southern region includes (12) districts.

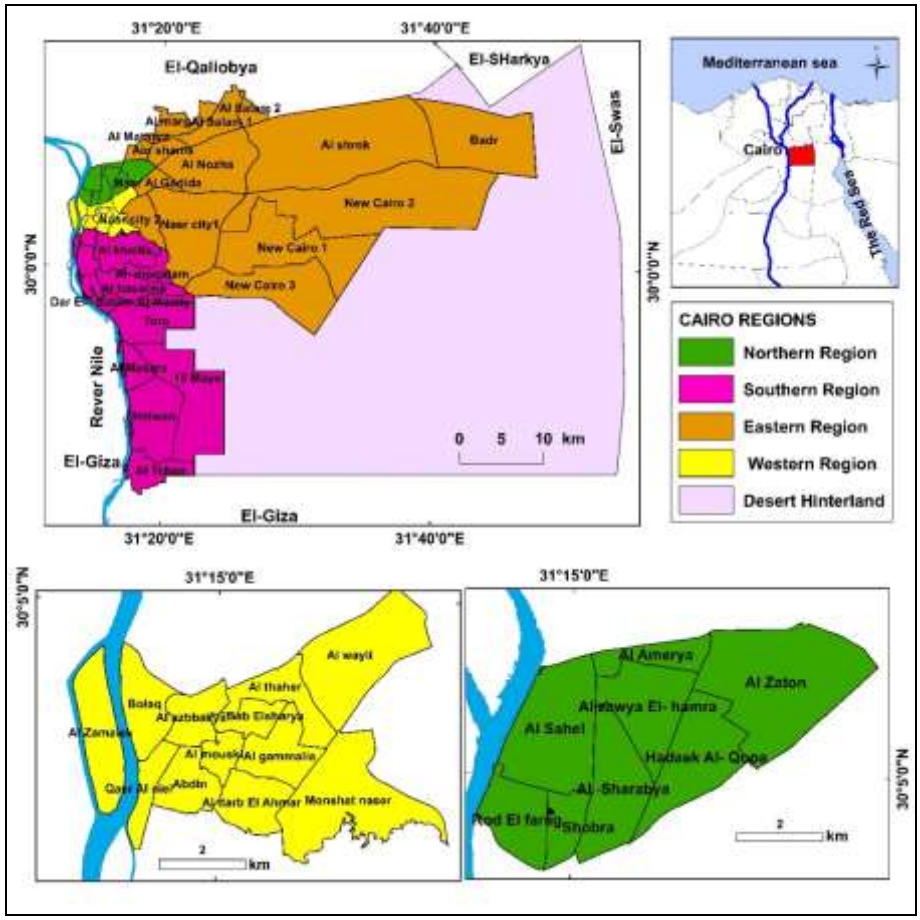

Figure 1. Map of the study area (location and administration).

2.2 Data Collection

Data of COVID −19 cases during study period, From 14 February 2020 to 18 of May 2021, was collected from the Egyptian Ministry of Health and Population **(MOHP)**. To estimate the Morbidity of COVID-19 for each Shiakha, the population data estimated Morbidity rates "cases/100000 population" of Cairo were obtained by the Central Agency for Public Mobilization and Statistics, Egypt. The total number of conformed cases, recovered and deaths from COVID-19 provided by **(MOHP)** which were further used for spatial analysis. Cumulative Morbidity rate reveals the percentage of a population who gets sick in a specific duration of time. The spatial patterns of these cases were analyzed by a Geographical Information Systems (GIS) approach applying ArcGIS software, version 10.3.1 to create a spatial database and to analyze the spatial distribution of officially reported COVID-19 cases.

2.3 Statistical Analysis of COVID-19

Measuring spatial autocorrelation is an important method for quantitative analyses in geography. This method can be treated as a cornerstone of spatial statistics. Spatial analysis is essential to understand the spatial spread of infection and its association with the community and environment, especially in the early stages of an outbreak. Spatial autocorrelation was studied by Global Moran's I (Moran, 1950), Local Moran's I according to Anselin (1995) and Getis-Ord General G.

2.3.1 Spatial Clustering Analysis

Spatial autocorrelation was applied to assess the spatial correlation between variables through matching location similarity and attribute similarity (Huo et al., 2012). **Global Moran's I**, an index of spatial autocorrelation based on cross products is mathematically expressed as follows:

$$I = \frac{\sum_{i=1}^{n}\sum_{j=1}^{n} w_{ij}(x_i - \bar{x})(x_j - \bar{x})}{\sum_{i=1}^{n}(x_i - \bar{x})}$$

Where n is the number of regions; xi the attribute value at area I; $\bar{x}$ the mean value of the attribute in the study region; and wij element of a spatial lag operator W (spatial weights of matrix W). The significance of the index is usually tested in a situation of normal distribution (Mazzulla et al., 2012). Global Moran's I varies between-1 and 1 with a positive value meaning that a point in question is prone to be clustered by adjacent points, while a

negative value means the opposite. Values close to 0 indicate that the data is randomly distributed. **Local Moran's I analysis** (Anselin, 1995) was applied to identify statistically significant hotspots, cold spot and outliers. Local Moran's I is expressed by the following formula:

$$I_{\mathrm{i}} = x_i \sum_j w_{ij} x_j$$

The variables and calculation of the Local Moran's *I* are thus similar to those of Global Moran's *I*. It is possible to acquire the mean and the variance of *Ii* based on randomization, and inference can be carried out by normalized statistic with Z-score and *p*-value indicating statistical significance. The different classes of z-values are represented as High-High (HH) or Low-Low (LL). High, positive z-values indicate that an area is surrounded by areas have similar values. Conversely, a low negative z-score indicates a statistically significant spatial anomaly, *i.e*. a high-value area surrounded by low-value areas (HL) with a LH area representing the inverse (Huo et al., 2011; Samphutthanon et al., 2013).

2.3.2 Getis-Ord General G

Local spatial autocorrelation explores within the global pattern to recognize clusters (hot spots) that either drives the overall clustering, or that shows heterogeneities that depart from global pattern (Ord and Getis, 2001). Local hot spot analysis tool (Getis-Ord Gi*) used to explore the spatial gathering hotspots and cold spots of the COVID-19 pandemic in Cairo. The Getis-Ord Gi* Index is defined as:

$$G_i^* = \frac{\sum_{\mathrm{j}=1}^{n} w_{i,j} x_j - \bar{x} \sum_{j=1}^{n} w_{i,j}}{S \sqrt{\frac{\left[n \sum_{j=1}^{n} w_{i,j}^2 - \left(\sum_{j=1}^{n} w_{i,j} \right)^2 \right]}{n-1}}}$$

Where n is the number of spatial units that need to be analyzed, xi and xj are the attribute values of the COVID-19 confirmed case in locations i and j, respectively, Wij is the spatial weight between elements i and j, and x is the average value of the attributes and S is the standard deviation.

3. Results

3.1 Analysis of COVID-19 pandemic in Cairo

3.1.1 Mapping the distribution of COVID-19

The Morbidity and fatality rates of Covid-19 in the (46) districts provinces in Cairo as can be seen from Table (1) and Figure (2), depicting the situation during the study period, (From 14 February 2020 to 18 of May 2021), the top five districts with respect to cases number of Covid19 were the following provinces: Nasr city (5466), Helwan (3882), Bolaq (3093), Al Sayeda Zainab (3015) and Al Khalifa (2975). Moreover, the districts with the highest Morbidity rate were Al- Mouski (0.097/100000), Badr (0.088/100000), Qasr Al-Niel (0.088/100000), Al Gammalia (0.066/100000) and Al Zamalek (0.064/100000), Figure (3).

Table 1. Morbidity and fatality rate of Covid-19 in Cairo regions.

Region	district	total population	Confirmed cases	Coved-19 Morbidity (per 100000)	Fatality cases	Percentage of fatality
Northern Region	Rod El farag	148353	1414	0.010	164	0.12
	Monshat naser	263187	1357	0.005	267	0.20
	Bab Elsharya	47541	1253	0.026	184	0.15
	Al thaher	73212	1207	0.016	131	0.11
	Al azbbakya	20132	1196	0.059	136	0.11
	Al shrok	88909	1194	0.013	114	0.10
	15 Mayo	95313	1163	0.012	96	0.08
	New Cairo 2	92360	1085	0.012	114	0.11
Total		**829007**	**9869**	**0.012**	**0.012**	**0.11**
Southern Region	Nasr city 1	646634	5466	0.008	505	0.09
	Helwan	530967	3882	0.007	362	0.09
	Bolaq	49046	3093	0.063	294	0.10
	Al Sayeda Zainab	138826	3015	0.022	307	0.10
	Al khalifa	107197	2975	0.028	283	1.75
	Masr El qadima	254980	2867	0.011	246	0.09
	Badr	31877	2818	0.088	276	0.10
	Al wayli	80774	2516	0.031	248	0.10
	Al gammalia	37045	2453	0.066	342	0.14
	Al marg	813529	2236	0.003	185	0.08
	Al basatine	504659	2231	0.004	218	0.10
	Nasr city 2	73523	2106	0.029	210	0.10
Total		**3269057**	**35658**	**0.011**	**0.011**	**0.10**

Table 1. (Continued) Morbidity and fatality rate of Covid-19 in Cairo regions.

Region	district	total population	Confirmed cases	Coved-19 Morbidity (per 100000)	Fatality cases	Percentage of fatality
Eastern Region	Al darb El Ahmar	59578	2033	0.034	249	0.12
	Ain shams	625848	1890	0.003	171	0.09
	New Cairo 3	72203	1825	0.025	165	0.09
	Tora	234559	1813	0.008	152	0.08
	Al mouski	16973	1649	0.097	206	0.12
	Abdin	41076	1629	0.040	192	0.12
	Al Teben	73385	1623	0.022	121	0.07
	Al Matarya	613709	1597	0.003	178	0.11
	Al Sahel	322323	1551	0.005	169	0.11
	Hadaek Al- Qopa	321968	1550	0.005	156	0.10
	New Cairo 1	138363	1525	0.011	148	0.10
	Al Nnozha	235557	1499	0.006	124	0.08
	Masr Al Gadida	136619	1468	0.011	122	0.08
	Al Salam 1	489674	1432	0.003	102	0.29
Total		**3381835**	**23084**	**0.007**	**0.007**	**0.11**
Western Region	Al Zaton	177431	1066	0.006	109	0.10
	Al -moqatam	228316	1058	0.005	111	0.68
	Al Masara	275071	1023	0.004	94	0.28
	Al -Sharabya	190695	1000	0.005	78	0.08
	Al Maady	90231	996	0.011	91	0.09
	Al Zamalek	15225	977	0.064	129	0.13
	Qasr Al niel	10760	949	0.088	75	0.08
	Dar El– Salam	525638	924	0.002	79	0.26
	Shobra	78128	864	0.011	98	0.11
	Al zawya El- hamra	324107	734	0.002	34	0.05
	Al Amerya	155402	367	0.002	17	0.05
	Al-Salam 2	156633	331	0.002	37	0.11
Total		**2227637**	**10289**	**0.005**	**0.005**	**0.17**
Desert Hinterland		**310087**	**230**	**0.001**	**0.001**	**0.17**
Total Cairo		**10017623**	**79130**	**0.008**	**0.008**	**0.16**

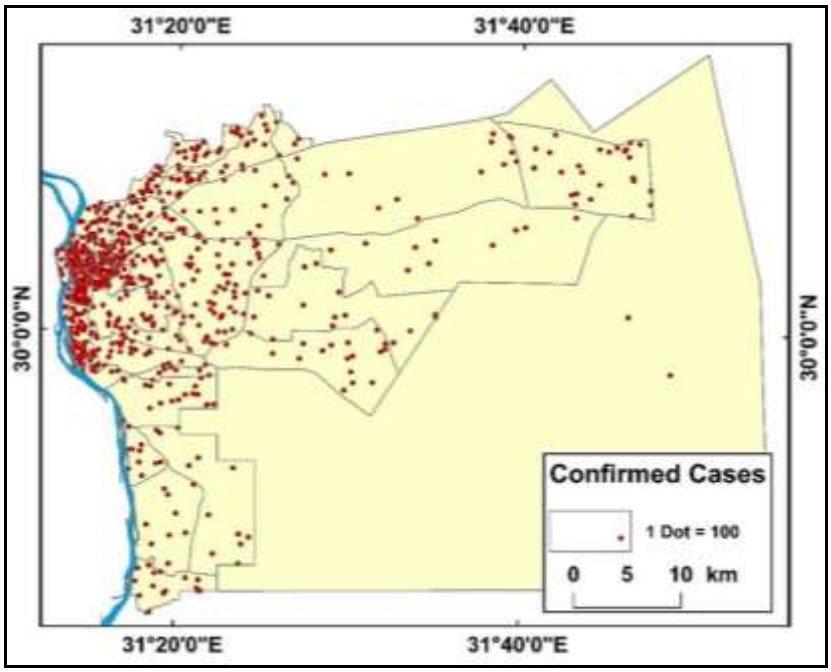

Figure 2. Geographical disribution of cumulative confirmed COVID-19 cases in Cairo from 14 February 2020 to 18 of May 2021.

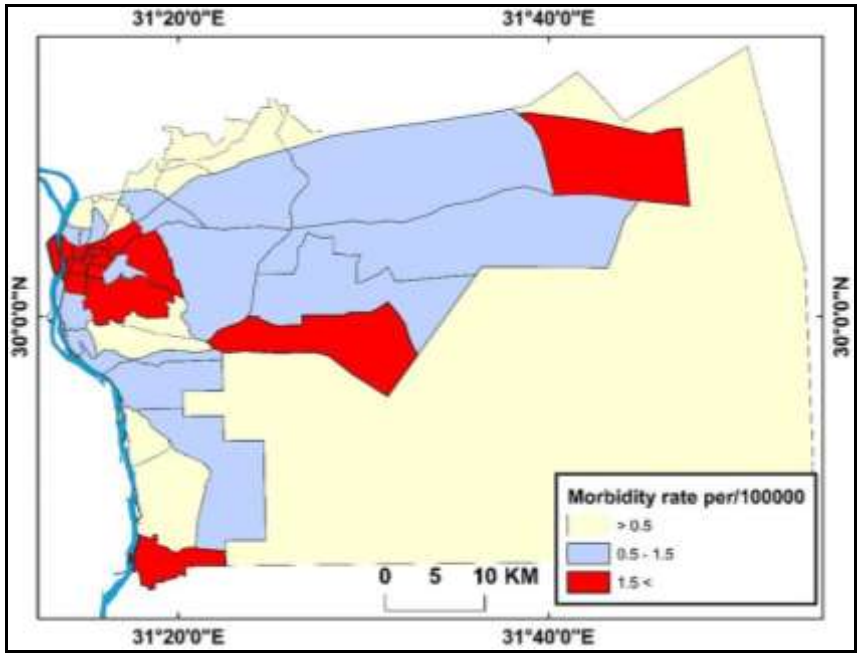

Figure 3. Morbidity rate of COVID-19.

3.2 Mapping Population Density

Population density has been used as a surrogate measure of social distancing capacity and study has shown that COVID-19 transmission is potentially more likely to occur among districts with higher population densities as can be seen from the map of population density in Cairo, figure (4).

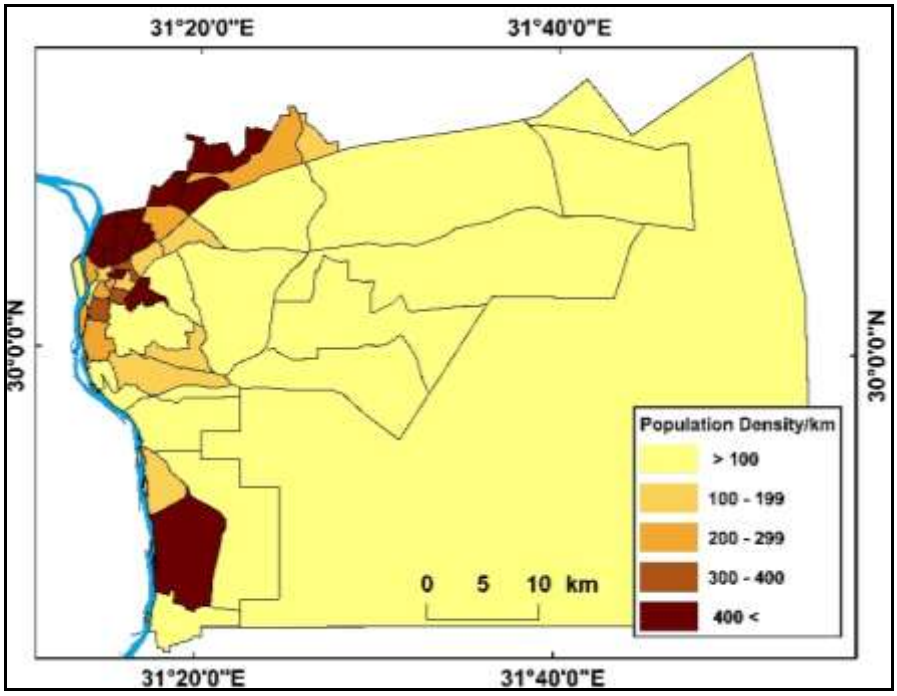

Figure 4. Population density.

3.3 Analyses of Spatial Patterns

3.3.1 Global Spatial Cluster Analysis

Here, a spatial autocorrelation statistical model is used to conduct a global autocorrelation test of the significance of the Moran's I index on the COVID-19 outbreak data of Cairo From 14 February 2020 to 18 of May 2021. Cairo 46 administrative regions were greater than zero (positive) for Covid-19 according to Global Moran's I calculations (Figure 5-A). Moran's I and the z-score were 0.525915 ($p=0< 0.01$), 15.856186, respectively, indicating that the **morbidity of Covid-19** was significant positive spatial autocorrelation and spatially clustered between regions in Cairo COVID-19 pandemic. It can be found that the Moran's I index for **recovery cases** of Covid-19 Moran's I = (0.499273) is greater than zero. The z-score is 15.05645 and $p < 0.01$ (Figure 5-B), indicating that there is a significant

positive spatial autocorrelation, and Moran's I index for Covid-19 fatality **cases** (Moran's I = 0.370994) is greater than zero. The z-score is 11.22548 and $p < 0.01$(Figure 5-C), indicating that there is a significant positive spatial autocorrelation also.

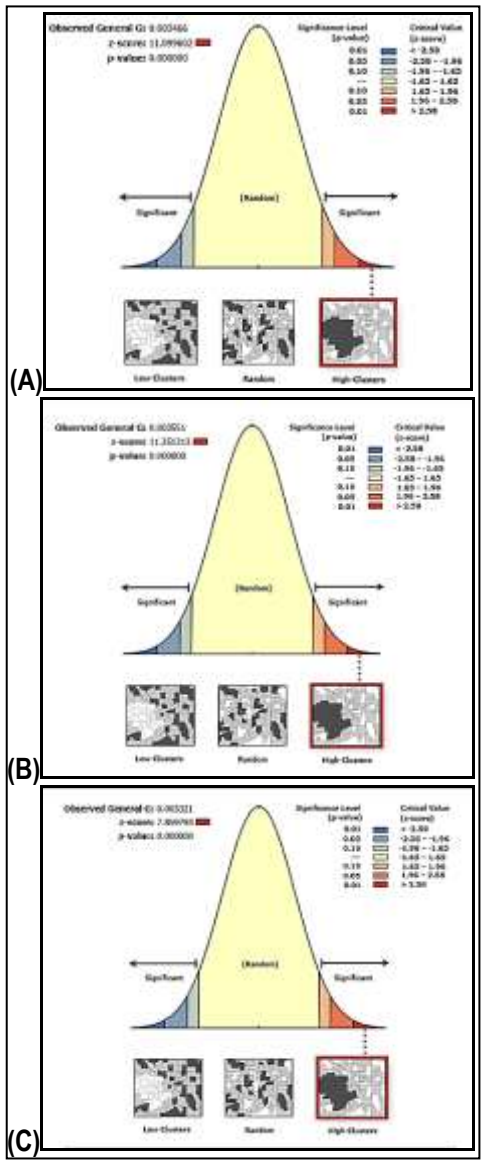

Figure 5. Global spatial autocorrelation analysis of Covid-19 (global Moran's I index).

3.3.2 Local Spatial Cluster Analysis

Local spatial cluster analysis used to reveal the correlation between the spatial geographical unit and its adjacent spatial unit attribute feature values, and to identify 'hot spots' and heterogeneity test of their data. The results of Local Moran's I analysis for the morbidity cases reveals that the value of 71 sheikhs belonging to the HH aggregation class. Eastern, Northern and southern Cairo were found to be the major High morbidity cluster of COVID-19, while western Cairo was identified as Low morbidity clusters. The Covid-19 morbidity in Cairo shows that the current COVID-19 pandemic has developed hotspots (HH) and cold spots may develop (LL). The results are shown in Figure (6). A Similar clusters pattern was observed for the recovery cases as displayed in Figure (7) indicating that Cairo has a highly recovery rate of COVID-19. Cluster analysis of fatality cases, showed Eastern and Southern Cairo as high fatality cluster of COVID-19 while Northern and western Cairo were identified as Low fatality clusters as displayed in Figure (8).

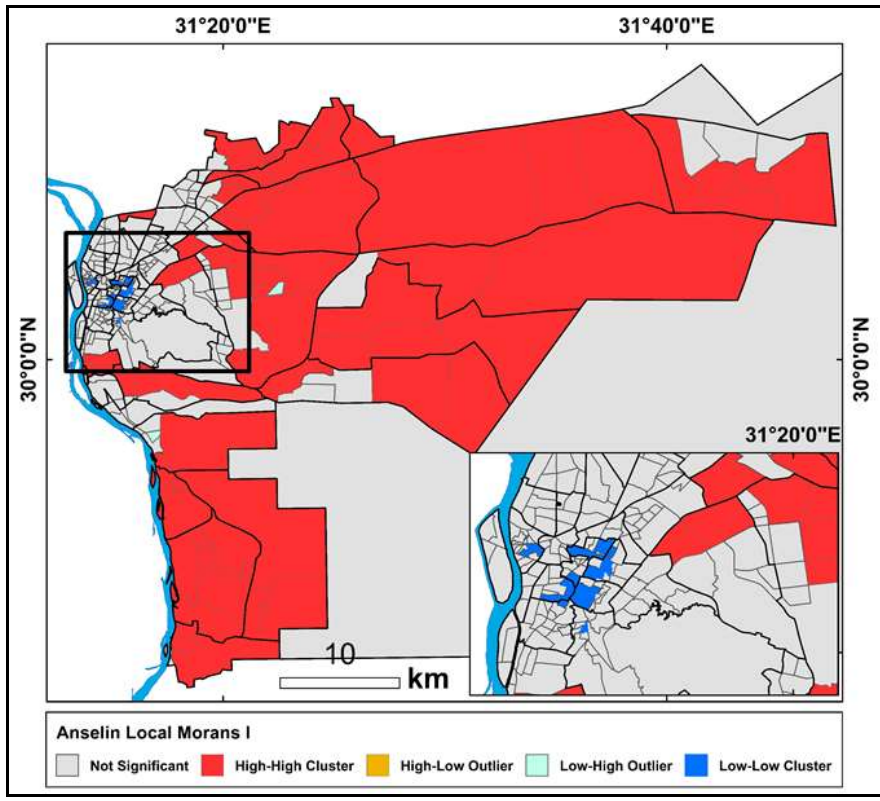

Figure 6. Local spatial autocorrelation analysis of COVID-19 morbidity cases.

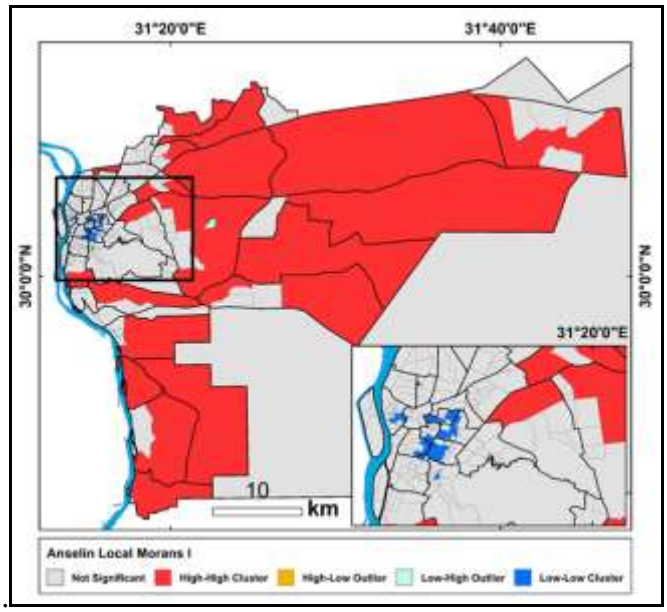

Figure 7. Local spatial autocorrelation analysis of COVID-19 recovery cases.

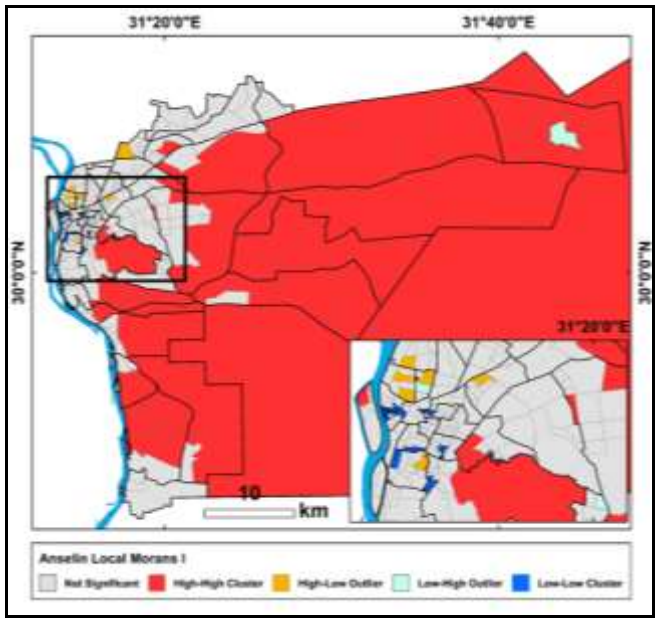

Figure 8. Local spatial autocorrelation analysis of COVID-19 fatality cases.

3.3.3 Hot Spot Analysis

To identify COVID-19 hot-spots, the Getis -OrdGi statistic was applied and the results are depicted in Figure 7. The clustering of high values (hot spots) for morbidity were distributed with a confidence level of 99% in eastern, southern and northern east of Cairo while the indicator detected clustering of low values (cold spots) in the central part of the western region of Cairo with a confidence level of 99% as demonstrated in Figure (9). The clustering of the cold spot with a confidence level of 95% and 90%was distributed around the central part of western region ,similar clustering distribution of the hot spot and cold spot were observed for the recovery and fatality cases as displayed in Figures (10) & (11). The spread of the COVID-19 virus is affected by some factors (Lin et al., 2020) such as higher population density and population movement which may lead to higher COVID-19 infections (Ahmadi et al., 2020).

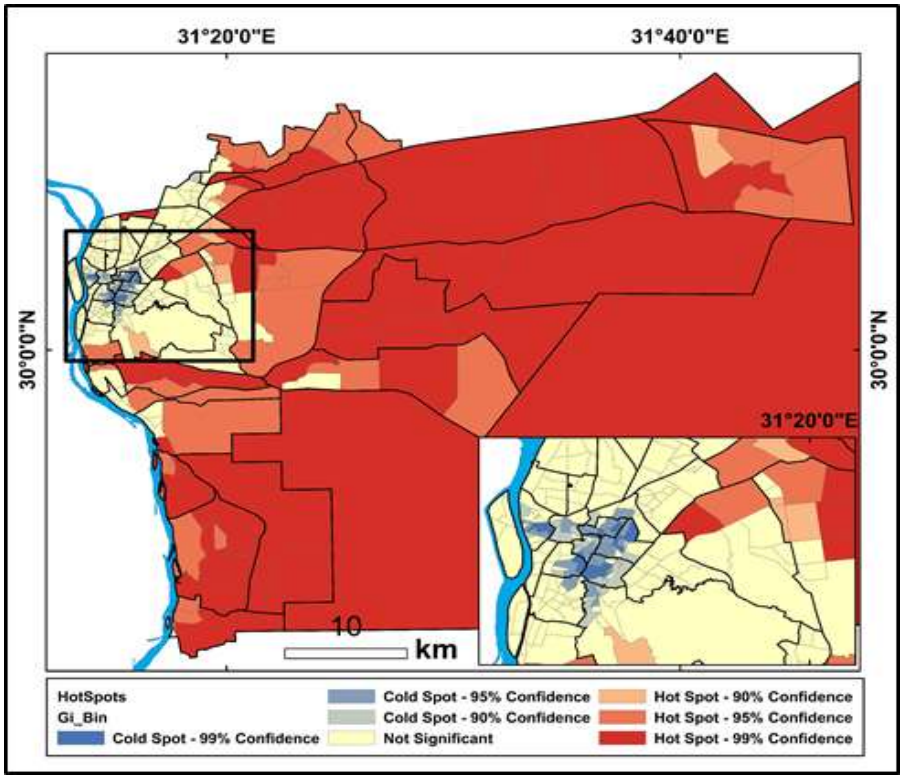

Figure 9. Hot-spot map of COVID-19 morbidity cases in Cairo.

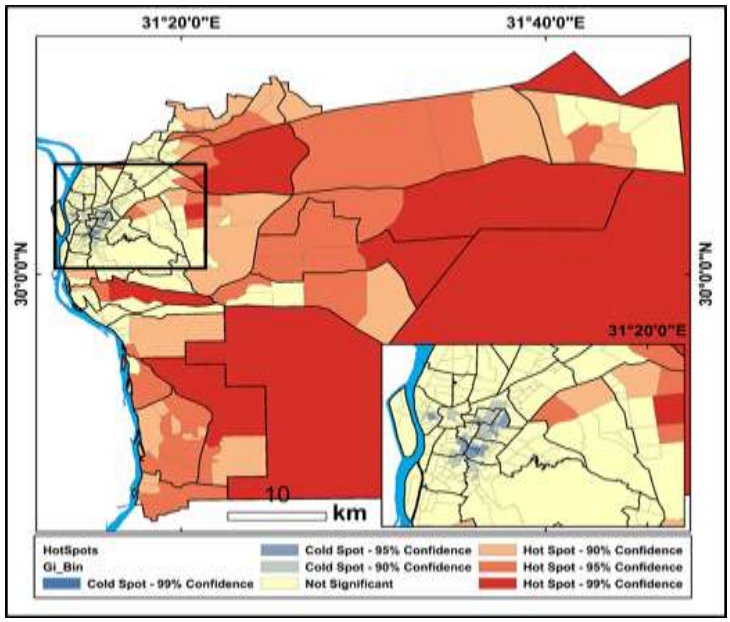

Figure 10. Hot-spot map of COVID-19 recovery cases in Cairo.

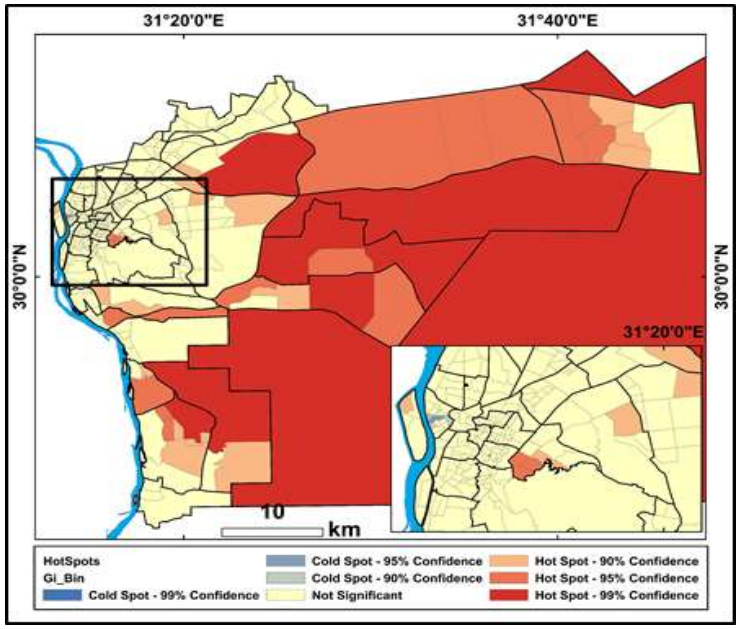

Figure 11. Hot-spot map of COVID-19 fatality cases in Cairo.

4. Discussion

The COVID-19 pandemic in Cairo is a part of the worldwide pandemic of coronavirus disease (COVID-19). Egypt's health ministry announced the first case in the country at Cairo International Airport on 14 February 2020. This study As far as we know is the first study that maps vulnerability to COVID-19 morbidity, recovery cases and associated fatality in Cairo at a high resolution.This study aims to analyze the reported Covid-19 incidence by spatial statistical methods, exploring the geographical distribution of the disease. The spatial autocorrelation (global Moran's I) during the study period showed that the Morbidity rate , recovery and fatality of COVID19 in the study area was in the clustering pattern, and there was less than 1% likelihood that this clustering pattern could be the result of random chance. While local spatial correlation analysis showed that the value of 71 locations belonging to the HH aggregation class because these areas have high population density. Eastern and southern Cairo was found to be the major High morbidity cluster of COVID-19, while western Cairo was identified as Low morbidity clusters. Answers to the questions whether the disease will stay in the same geographic location or spread to nearby areas, and whether the measures applied to contain further spread are effective, require HL cluster analysis extended over a longer time. Hot spot analysis (Getis-Ord GI) is considered as a helpful tool to recognize spatial clusters of both high and low values, and has previously been applied to model several disease outbreaks (Martin et al., 2011; Firestone et al., 2012). Following identifying the districts in the hot spots' area, preventive measures should be taken to halt the further spreading of the virus in neighboring districts and governorates, especially those located in cold spots. There is also a need to evaluate the influencing factors such as environmental, climatic, etc. components that have caused the formation of hot spot clusters in these districts. Our study also showed that the risk for severe cases of COVID-19 infection is high in the most parts of Cairo. This may be due to the high prevalence of population density in the capital. Population mobility could be regarded as a factor that led to the spread of the disease. The high infection rate in Cairo at this initial stage is expected, given that Cairo is a major travel hub and Bole International Airport, located in the governorate, is one of the largest international airports in Africa. This exposes Cairo to a higher risk of imported cases and, subsequently, to an early surge of infections, leaving the areas outside the governorate at a higher risk of later infection. Besides, epidemiological and virological data suggests that COVID-19 is primarily transmitted to contacts through respiratory droplets, virus-contaminated objects and surfaces. In the absence of effective human intervention, environmental factors and climate (such as humidity and wind direction) may spur the spread of the pandemic (Lin et al., 2020; Ward et al.,

2020). Some recent studies also indicate that temperature, humidity and wind speed may affect the morbidity rate of COVID-19 (Ahmadi et al., 2020; Ma et al., 2020). Therefore, climate factors related to the spread of the virus should be considered for some controlled measures. There are differences in climatic conditions in different regions and areas with high humidity are at greater risk of virus transmission. Control measures should be strengthened. The possibility of airborne transmission of the virus also needs to be considered in COVID-19 prevention and control. During an pandemic, population density in public places (supermarkets, shopping malls) and public transport (subway, bus) should be controlled, and the risk of spread of the disease should be reduced by frequent disinfection and wearing masks. In order to contain the spread of the virus, Egypt suspended schools and universities for one month and encouraged electronic distance learning. Also, Egypt imposed a curfew from 7 pm until 6 am, during which all shops and markets are closed from 5 pm to 6 pm and are subjected to a complete shutdown on Fridays and Saturdays. Besides, all means of public and private transportation are suspended during curfew hours. Flight into or out of Egypt were also suspended in an attempt to reduce the risk of importing infection. All sports and many social activities were also banned to prevent the spread of COVID-19. (Medhat, M. A., et al., 2020) Egypt abandoned individual hospitals in every governorate to be assigned as quarantine hospitals for COVID-19 patients. Egyptian Ministry of Health and Population **(MOHP)** decided to relay on a medical team composed of different specialties to take care of the inpatients in these quarantine hospitals (Medhat, M. A., et al., 2020). Depending on Egypt's situation on the WHO official website https://covid19.who.int/region/emro/country/eg, there have been **325,508** confirmed cases of COVID-19 and **18,333** coronavirus-related deaths reported in the country since the pandemic began until 23 October 2021. Egypt has administered at least **9,391,465** doses of COVID vaccines so far. Assuming every person needs 2 doses, that's enough to have vaccinated about **4.7%** of the country's population. As of 23 October 2021, a total of 25,083,832 vaccine doses have been administered.

5. Conclusions

- COVID-19 is characterized by a long incubation period, strong infectivity and difficulty of detection, which has led to the sudden outbreak and the rapid spread of an pandemic. This situation requires GIS and big data technology to allow rapid responses and analyses, a quick supply of information about the pandemic dynamics and an understanding of the pandemic spread rules to provide timely support for the prevention and control decisions and actions.

- This study depended on the preparation of new geodatabase for the COVID-19 pandemic based on the COVID-19 pandemic available data and using ArcGIS spatial statistics methods to analyze spatial patterns of the COVID-19 pandemic and explored the correlation analysis from 14 February 2020 to 18 of May 2021.
- Hotspot analysis coupled with Anselin local Moran'sI provides a scrupulous and objective approach to determine the locations of statistically significant clusters of COVID-19 cases shedding light on the high-risk districts. The study offers maps that can guide the targeted interventions necessary to contain the spread of COVID-19 in Cairo.

6. Recommendations

This study identified the provinces with high and low Covid19 clusters in Cairo. Spatial correlations between districts may provide instructive information for the control of Covid-19 pandemic in Cairo. Follow-up HL cluster analysis with a longer time perspective is advised.

7. Author contribution

The authors confirm contribution to the paper as follows: study conception and design: Second. Author; data collection and methodology: First. Author; Geodatabase Preparation: All. Authors; analysis and interpretation of results: Second. Author; draft manuscript preparation: First. Author. All authors reviewed the results and approved the final version of the manuscript.

8. Acknowledgements

All thank to the people who were struggling in the healthcare fields to overcome the COVID-19 outbreak.

9. Declarations

Authors declare that no potential conflicts of interest with respect to the research, authorship, and/or publication of this article.

References

1. Ahmadi, M., Sharifi, A., Dorosti, S., Ghoushchi, S. J. & Ghanbari, N. 2020, "Investigation of effective climatology parameters on COVID19 outbreak in Iran". Science of the Total Environment, vol. 729, pp. 1–7. https://doi.org/10.1016/j.scito tenv.2020.138705
2. Anselin, L. 1995, "Local Indicators of Spatial Association—LISA", Geographical analysis, vol. 27, no. 2, pp. 93-115.

3. Bivand, R. 2014, "Spatial dependence: weighting schemes, statistics and models", version 0.5-37 pp.1-200. URL http://CRAN.R-project.org/package.
4. Cucinotta, D., Vanelli M. (2020)," WHO declares COVID-19 a pandemic", Acta Biomed, vol. 91, pp.157-160.
5. Firestone, S., Christley, R., Ward, M., & Dhand, N. 2012, "Adding the spatial dimension to the social network analysis of an epidemic: Investigation of the 2007 outbreak of equine influenza in Australia", Preventive veterinary medicine, vol. 10, pp.123-135. doi: 10.1016/j.prevetmed.2012.01.020.
6. Franch,P., Napoletano, B., Rosete, F. & Billa, L. 2020, "Spatial analysis and GIS in the study of COVID-19. A review", journal Science of The Total Environment, vol. 739, pp.1-10. https://doi.org/10.1016/j.scitotenv.2020.140033.2020.140033.
7. Huo, X., Li, H., Sun, D., Zhou, L. & Li, B. 2012, "Combining Geostatistics with Moran's I Analysis for Mapping Soil Heavy Metals in Beijing, China", International journal of environmental research and public health. vol. 9, no. 3, pp. 995-1017.
8. Huo, X., Zhang, W., Sun, D., Li, H., Zhou, L. & Li, B. 2011, "Spatial Pattern Analysis of Heavy Metals in Beijing Agricultural Soils Based on Spatial Autocorrelation Statistics". International journal of environmental research and public health. vol. 8, no. 6, pp. 2074 -2089. doi:10.3390/ijerph8062074.
9. Jun, L., Weihao, H., Muchen,W., Dehong, Li., Shuyi, M., Jiawen, H., Hang ,H., Shan ,Y., Yanjun, Q., Peiling, C., Qiao, Z., Ningbo ,Y. & Shaolong S. 2020, "Containing the spread of coronavirus disease 2019 (COVID-19): Meteorological factors and control strategies", Science of The Total Environment, vol. 744, pp. 1-7. https://doi.org/10.1016/j.scitotenv.2020.140935
10. Martin, V., Pfeiffer, D.U., Zhou, X., Xiao, X., Prosser, D.J., Guo, F. & Gilbert, M. 2011," Spatial distribution and risk factors of highly pathogenic avian influenza (HPAI) H5N1 in China:, PLoS pathogens, vol. 7, no. 3, pp. 1-11. https://doi.org/10.1371/journal.ppat.1001308
11. Martins, M., Francisco, R., Pinheiro, M., Ramos J, A., Alencar, C., Bezerra, F & Heukelbach, J. 2015," Spatiotemporal Patterns of Schistosomiasis-Related Deaths, Brazil, 2000–2011", Emerging Infectious Diseases. Vol. 21, pp. 1820-1823. doi:10.3201/eid2110.141438
12. Mazzulla, G. & Forciniti, C. 2012," Spatial association techniques for analysing trip distribution in an urban area", European Transport Research Review, vol. 4, pp. 217-233. doi:10.1007/s12544-012-0082-9.
13. Medhat, M.A. & El Kassas, M. 2020, "COVID-19 in Egypt: Uncovered figures or a different situation?", Journal of global health, vol. 10, no. 1, pp. 1-4. https://doi.org/10.7189/jogh.10.010368
14. Mohamed, I.K. 2020," A view of the health services after COVID-19: an Egyptian perspective", Alexandria Journal of Medicine, vol. 56, no. 1, pp. 118-129. https://doi.org/10.1080/20905068.2020.1789391
15. Moran PAP. 1950, "Notes on Continuous Stochastic Phenomena". Biometrika, vol. 371, pp.17-23. doi:10.2307/2332142. JSTOR2332142.

16. Ord, K., Getis, A. 2001, "Testing for Local Spatial Autocorrelation in the Presence of Global Spatial Autocorrelation", Journal of Regional Science, vol. 41, pp. 411-432. doi:10.1111/0022-4146.00224.
17. Pattison, W.D., 1964. "The four traditions of geography". Journal of Geography, vol. 63 , pp. 211–216.
18. Robertson, C. & Nelson, T. A. 2014, "An overview of spatial analysis of emerging infectious diseases", The Professional Geographer, vol. 66, no. 4, pp. 579–588.
19. Sauer, C.O., 1925, "The Morphology of Landscape", University of California, Oakland, CA, USA, vol. 2, pp. 19–53.
20. Shariati, M., Mesgari, T., Kasraee, M. 2020. "Spatiotemporal analysis and hotspots detection of COVID-19 using geographic information system (March and April, 2020". Journal of Environmental Health Science and Engineering. vol.18, pp**.** 1499–1507. https://doi.org/10.1007/s40201-020-00565-x.
21. Subramanian, S. V., Karlsson, O., Zhang, W. & Kim, R. 2020, "Geo-mapping of COVID-19 risk correlates across districts and parliamentary constituencies in India", Harvard Data Science Review. Special Issue 1‹COVID-19: Unprecedented Challenges and Chances pp.1-35. https://doi.org/10.1162/99608f92.68bb12e4 .
22. Turner, B.L. 2002, "Contested identities: human-environment geography and disciplinary implications in a restructuring academy" , Annals of the association of american geographers. vol. 92, no.1, pp.52–74.
23. Werneck, G. L. 2008, "Georeferenced data in epidemiologic research", Cieˆncia&Sau´deColetiva, vol.13(6), pp. 1753–1766.
24. WHO 2020.Coronavirus disease (COVID-19): situation report. Weekly Operational Update on COVID-19 25 September 2020. pp.1-13
25. https://covid19.who.int/region/emro/country/eg
26. http://www.cairo.gov.eg/en/Pages/CairoInLines.aspx?CiLID=9

التحليل الجغرافى لإنتشار فيروس كوفيد-١٩ بمحافظة القاهرة
باستخدام نظم المعلومات الجغرافية

الملخص

تسبب فيروس كورونا المستجد (كوفيد-١٩) في أزمة صحية عامة عالمية أثرت على معظم البلدان بما في ذلك مصر. ونظرًا لتفشي الجائحة، جذب تطور كوفيد-١٩ اهتمامًا عالميًا متزايدًا. وتهدف هذه الدراسة إلى تحديد ورصد الانتشار المكانى للجائحة اعتماداً على استخدام اساليب التحليل الإحصائى لحالات الإصابة المُبلغة بكوفيد-١٩ فضلا عن استكشاف أنماط التوزيع الجغرافي لجائحة كوفيد-١٩ بالقاهرة في الفترة من ١٤ فبراير ٢٠٢٠ إلى ١٨ مايو ٢٠٢١. ومن أجل فهم أفضل لانتشار هذا الفيروس المستجد، تم تمييز الأنماط المكانية للحالات التراكمية للإصابة بكوفيد-١٩ باستخدام برنامج ArcGIS v.10.3.1 لتطبيق تحليل الارتباط المكاني التلقائي وتحديد نمط التوزيع الجغرافي من خلال تطبيق مؤشرموران العالمى Global Moran's I، كما تم تطبيق مؤشرموران المحلى Local Moran's I، ومؤشر البقع الساخنة Getis-Ord Gi لاستكشاف البقع الساخنة والباردة للتجمع المكاني لجائحة كوفيد-١٩. أبلغت محافظة القاهرة عن ٧٩١٣٠ حالة اصابة بكوفيد-١٩ وذلك حتى ١٨ مايو ٢٠٢١ واحتلت الأقسام الآتية المراكز الخمس الأولى من حيث ارتفاع معدل الإصابة والذى بلغ نحو (١٠٠٠٠٠/٠.٠٩٧) بالموسكي و(١٠٠٠٠٠/٠.٠٨٨) ببدر و(١٠٠٠٠٠/٠.٠٨٨) بقصر النيل و(١٠٠٠٠٠/٠.٠٦٦) بالجمالية و(١٠٠٠٠٠/٠.٠٦٤) بالزمالك، وأظهرت نتائج تحليل موران العالمى أن معدل الإصابة والتعافي والوفاة من كوفيد-١٩ كان في نمط التجميع High clustered، وان هناك احتمال أقل من ١٪ أن يكون هذا النمط العنقودي نتيجة للصدفة العشوائية. بينما أظهر تحليل الارتباط المكاني المحلي أن قيم ٧١ شياخة تنتمي إلى فئة تجميع High High cluster "يعزو ارتفاع معدل الاصابة بهذه المناطق للكثافة السكانية المرتفعة". وأظهرت نتائج تطبيق مؤشر Getis-OrdGi أن تجمع القيم العالية التي تمثل البقع الساخنة توزعت في شرق وجنوب وشمال شرق القاهرة بمستوى ثقة ٩٩٪.

الكلمات المفتاحية: كوفيد ١٩، نظم المعلومات الجغرافية، الارتباط المكاني التلقائي، البقع الساخنة/الباردة، القاهرة.